

Interpreting a 750 GeV Diphoton Resonance

Rick S. Gupta,^a Sebastian Jäger,^{a,b} Yevgeny Kats,^a Gilad Perez,^a Emmanuel Stamou^a

^a*Department of Particle Physics and Astrophysics, Weizmann Institute of Science,
Rehovot 7610001, Israel*

^b*Department of Physics and Astronomy, University of Sussex,
Brighton, BN1 9QH, UK*

E-mail: rsgupta@weizmann.ac.il, S.Jaeger@sussex.ac.uk,
yevgeny.kats@weizmann.ac.il, gilad.perez@weizmann.ac.il,
emmanuel.stamou@weizmann.ac.il

ABSTRACT: We discuss the implications of significant excesses in the diphoton final state observed by the LHC experiments ATLAS and CMS around 750 GeV diphoton invariant mass. Interpreting the result as a spin-zero s -channel resonance, the excess alone implies model-independent lower bounds on both the branching ratio and the coupling to photons, leading to stringent constraints on dynamical models. We consider both the case where the excess is described by a narrow and a broad resonance. We also obtain model-independent constraints on the allowed couplings and branching fractions to various other final states, by including the interplay with 8 TeV searches. These results can guide attempts to construct viable dynamical models of the resonance. Turning to specific models, our findings suggest that the anomaly cannot be accounted for by the presence of only an additional singlet or doublet spin zero field and the Standard Model degrees of freedom; this includes all Two-Higgs-doublet-models. We prove that the whole parameter space of the MSSM is ruled out as an explanation for the excess if the absence of charge and colour breaking minima is required. If we assume that the resonance is broad we find that it is challenging to find a weakly coupled explanation. However, we provide an existence proof in the form of a vectorlike model of quarks with exotic electric charge of 5/3 or above. For the narrow resonance case a similar model with ordinary charges can be perturbative up high scales. We also consider dilaton models, and they appear to be inconsistent with the data, even if arbitrary extra contributions to the QED and QCD beta functions are allowed. Prospects for the LHC run II and some implications for flavor physics are briefly discussed.

Contents

1	Introduction	1
2	Model-independent constraints	2
2.1	Implications of the excess alone	2
2.2	Interplay with previous LHC searches	5
3	Models	7
3.1	Extra SM gauge singlet	7
3.1.1	Renormalizable model with additional singlet	9
3.1.2	Boosting c_γ, c_g with new vectorlike fermions	9
3.2	The dilaton	12
3.3	Additional Pseudoscalar	13
3.4	Excluding the general 2HDM	14
3.4.1	Excluding the Pure 2HDM case	15
3.5	The fate of the MSSM	17
3.5.1	Constraints from vacuum stability	18
3.5.2	Conservative bounds on sfermion contributions	19
3.5.3	Contributions from other particles and verdict	21
4	Summary and Outlook	22

1 Introduction

Very recently, both the ATLAS and the CMS collaborations at CERN have reported mutually consistent ‘‘bumps’’ in the diphoton invariant mass distribution near 750 GeV [1, 2]. Based on 3.2 and 2.6 fb^{-1} of the 13 TeV LHC data, the corresponding deviations from the background-only hypothesis have local significances of 3.9σ and 2.6σ in ATLAS and CMS, respectively. The bumps, best described by relative width $\Gamma/M \approx 6\%$ in ATLAS [1] and sub-resolution width in CMS [2], are suggestive of a decay of a new particle beyond the Standard Model (BSM). The kinematic properties of the events in the excess region are reported not to show any significant deviations compared with events in sidebands. This disfavors significant contributions to the production from decays of yet heavier particles or associated production, and motivates focusing on the case of a direct production of a single 750 GeV resonance.

The purpose of the present paper is to characterise this theoretically unexpected result and discuss its implications for some leading paradigms for physics beyond the Standard Model. It is divided into two main parts, the first of which comprises a model-independent framework that aims to equip the reader with handy formulas for interpreting both the

signal and the most important resonance search constraints from existing LHC searches in the context of BSM models. We derive a number of bounds, including model-independent lower bounds on the branching ratio and partial width into photons of a hypothetical new particle. The second part investigates concrete scenarios, including the possibility of interpreting the resonance as a dilaton in theories of spontaneous breaking of scale invariance (or as the radion in warped extra dimension), or as a heavy Higgs scalar in a two-Higgs-doublet model. We find the properties of the observed resonance to be quite constraining. In particular, the interpretation as an s -channel resonance, if confirmed, falsifies the Minimal Supersymmetric Standard Model (MSSM) even under the most conservative assumptions about MSSM parameters and the true width of the resonance.

2 Model-independent constraints

We start by discussing what can be inferred about the new particle from data alone. We will first describe the implications of the observed properties of the diphoton bumps, and then examine the constraints from the absence of significant excesses in resonance searches in other final states that could be sensitive to other decay modes of the same particle.

2.1 Implications of the excess alone

Both ATLAS and CMS observe excesses in a diphoton invariant mass region of near 750 GeV. For the purposes of this note, we will generally assume the signal contribution to be $N = 20$ events for $\mathcal{L} = 5.8 \text{ fb}^{-1}$ integrated luminosity (adding up ATLAS and CMS), but we will make clear the scaling of our findings with N wherever feasible. We will also assume signal efficiency (including acceptance) of $\epsilon = 50\%$, even though in general it has some dependence on both the experiment and the details of the signal model.

The most straightforward signal interpretation is resonant s -channel production of a new unstable particle. The observed signal strength corresponds to a 13 TeV inclusive cross section to diphotons of

$$\sigma_{13} \times \text{BR}_{\gamma\gamma} \approx 6.9 \text{ fb} \times \left(\frac{N}{20} \right) \left(\frac{50\%}{\epsilon} \right) \left(\frac{5.8 \text{ fb}^{-1}}{\mathcal{L}_{13}} \right), \quad (2.1)$$

The diphoton final state precludes a spin-one interpretation due to the Landau-Yang theorem [3, 4], and we will henceforth assume spin zero. We take the mass to be $M = 750$ GeV; small variations have no significant impact on our findings. The shape of the excess in ATLAS may indicate a width of about $\Gamma = 45$ GeV [1]. However, we will also contemplate a smaller true width below, and discuss how our main findings depend on this.

To interpret the result and incorporate 8 TeV LHC constraints, a minimum of dynamical input is needed. The width-to-mass ratio is small enough to justify a narrow-width approximation to the level of accuracy we aim at here. In the narrow-width limit, resonant scattering amplitudes factorize into production and decay vertices, which we parameterize

mode	Width coefficient n_i	n_i (#)
$\gamma\gamma$	$\frac{1}{16(4\pi)^5}$	1.99×10^{-7}
gg	$\frac{1}{2(4\pi)^5}$	1.60×10^{-6}
$q_i\bar{q}_i$	$\frac{3}{8\pi}$	0.119
$t\bar{t}$	$\frac{3}{8\pi}\sqrt{1-4m_t^2/M^2}$	0.106
$\ell_i^+\ell_i^-$	$\frac{1}{8\pi}$	0.0398
hh	$\frac{1}{32\pi}\sqrt{1-4m_h^2/M^2}$	
WW	$\frac{1}{64\pi}\sqrt{1-4m_W^2/M^2}\frac{M^2}{m_W^2}\left[1-4\frac{m_W^2}{M^2}+12\frac{m_W^4}{M^4}\right]$	0.404
ZZ	$\frac{1}{128\pi}\sqrt{1-4m_Z^2/M^2}\frac{M^2}{m_Z^2}\left[1-4\frac{m_Z^2}{M^2}+12\frac{m_Z^4}{M^4}\right]$	0.154

Table 1. Width coefficients.

\sqrt{s}	[pb]	gg	$u\bar{u}$	$d\bar{d}$	$s\bar{s}$	$c\bar{c}$	$b\bar{b}$
13	$x_S^{13,p}$	$7.5 \cdot 10^{-3}$	250	150	14	9.8	4.4
8	$x_S^{8,p}$	$1.7 \cdot 10^{-3}$	95	57	3.7	2.3	0.96
13/8	r_p	4.4	2.6	2.7	3.9	4.2	4.6

Table 2. Leading-order production cross sections for a resonance with $M = 750$ GeV for $c_g = c_f = c_\gamma = 1$, using the PDF set `nn23l01`.

by terms in a “Lagrangian”

$$\mathcal{L} = -\frac{1}{16\pi^2} \frac{1}{4} \frac{c_\gamma}{M} \mathcal{S} F^{\mu\nu} F_{\mu\nu} - \frac{1}{16\pi^2} \frac{1}{4} \frac{c_g}{M} \mathcal{S} G^{\mu\nu,a} G_{\mu\nu}^a - c_W M_W \mathcal{S} W^{+\mu} W_\mu^- - \frac{1}{2} c_Z M_Z \mathcal{S} Z^\mu Z_\mu + \sum_f c_f \mathcal{S} \bar{f} f. \quad (2.2)$$

We emphasize that each term denotes a particular production and/or decay vertex and the parameterization \mathcal{L} does not make any assumptions about hierarchies of scales.¹

The total decay width of \mathcal{S} , ignoring contributions with quark loops, imposes one constraint on the couplings,

$$\frac{\Gamma}{M} = \sum_i \frac{\Gamma_i}{M} = \sum_i n_i c_i^2 + \frac{\Gamma_{\text{non-p}}}{M} \approx 0.06 \quad (2.3)$$

with the dimensionless coefficients n_i listed in Table 1 and with $\Gamma_{\text{non-p}}$ accounting for decay modes not explicitly included in the above Lagrangian, including invisible decays.

It is possible and convenient to represent the observed signal in terms of the branching ratios to the production mode and to $\gamma\gamma$. If a single production mode, p , dominates, the

¹In particular, the “couplings” c_i are on-shell form factors which generally include contributions from light particles and CP-even phases due to unitarity cuts. We discuss the connection to effective field theories in Section ??.

number of signal events, N , in the 13 TeV analyses fixes the product

$$\text{BR}_{\gamma\gamma} \times \text{BR}_p = n_p \frac{M}{\Gamma} \frac{N}{\epsilon x_S^{13,p} \mathcal{L}_{13}} = \kappa_p \times \left(\frac{N}{20} \right) \left(\frac{45 \text{ GeV}}{\Gamma} \right) \left(\frac{5.8 \text{ fb}^{-1}}{\mathcal{L}_{13}} \right) \quad (2.4)$$

where

$$\kappa_p \approx \{2.5, 5.5, 8.9, 96, 140, 310\} \times 10^{-5} \quad (2.5)$$

for the production modes

$$p = gg, u\bar{u}, d\bar{d}, s\bar{s}, c\bar{c}, b\bar{b}, \quad (2.6)$$

respectively, with $n_p = n_{gg}, n_{q_i\bar{q}_i}$ provided in table 1. We used the leading-order $\sqrt{s} = 13$ TeV production cross sections for $M = 750$ GeV,

$$\sigma_{13} = |c_p|^2 x_S^{13,p}, \quad (2.7)$$

where $x_S^{13,p}$ are listed in Table 2. A direct consequence of (2.4) is a lower bound on the branching ratio into photons,

$$\text{BR}_{\gamma\gamma} > \kappa_p \left(\frac{N}{20} \right) \left(\frac{45 \text{ GeV}}{\Gamma} \right) \left(\frac{5.8 \text{ fb}^{-1}}{\mathcal{L}_{13}} \right). \quad (2.8)$$

Note that this bound becomes more stringent if the width of the resonance is reduced.

Alternatively, the excess events fix the product of couplings

$$|c_\gamma c_p| = \sqrt{n_\gamma^{-1} \frac{\Gamma}{M} \frac{N}{\epsilon x_S^{13,p} \mathcal{L}_{13}}} = \rho_p \times \sqrt{\left(\frac{N}{20} \right) \left(\frac{\Gamma}{45 \text{ GeV}} \right) \left(\frac{5.8 \text{ fb}^{-1}}{\mathcal{L}_{13}} \right)}, \quad (2.9)$$

where

$$\rho_p \approx \{530, 2.9, 3.7, 12, 15, 22\}. \quad (2.10)$$

Since the couplings of the production modes, c_p , are bounded from above by the measured value of the width, c_γ cannot be arbitrarily small. For example, if a single production channel p dominates, one obtains

$$|c_\gamma| > \sqrt{\frac{n_p}{n_\gamma} \frac{N}{\epsilon x_S^{13,p} \mathcal{L}_{13}}} = \{2.7, 4.1, 5.2, 17.0, 20.5, 30.5\} \times \sqrt{\left(\frac{N}{20} \right) \left(\frac{5.8 \text{ fb}^{-1}}{\mathcal{L}_{13}} \right)}. \quad (2.11)$$

This result is independent of the width Γ .

In Figs. 1 and 2, we plot the general relation between $|c_\gamma|$ and $|c_p|$ for $N = 20$ expected excess events, switching on one production channel at a time. The mass and total width are fixed at 750 and 45 GeV, respectively. The partial widths to diphotons, $\Gamma_{\gamma\gamma}$ and to the production mode, Γ_p , are assumed to be supplemented by decays to other possible final states, $\Gamma_{\text{non-}p}$, to make up the total width. Contours of fixed $\Gamma_{\text{non-}p}$ are shown in dashed red. From the left panels of the Figures it is evident that for a given $\Gamma_{\text{non-}p}$ there exist two solutions, one for small and one for large c_γ . The lower bounds on c_γ in Eq. (2.11) are the crossings with $\Gamma_{\text{non-}p} = 0$ at the lower c_γ . From Fig. 1 we see that either large c_g or large c_γ is necessary to accommodate the excess. From this point of view, production via quark fusion, Fig. 2, relying on $c_f \lesssim 1$, might be considered a more natural possibility.

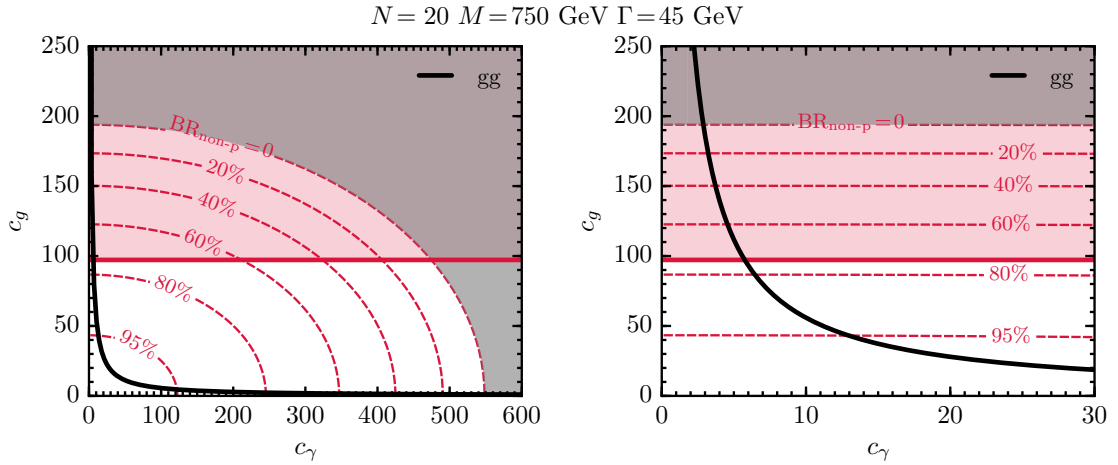


Figure 1. Points on black lines produce 20 signal diphoton events for a resonance with $M = 750$ GeV and $\Gamma = 45$ GeV when the resonance is produced 100% from gg . Red dashed lines are contours of fixed $\Gamma_{\text{non-p}}$. The right panel is a blowup of the left one.

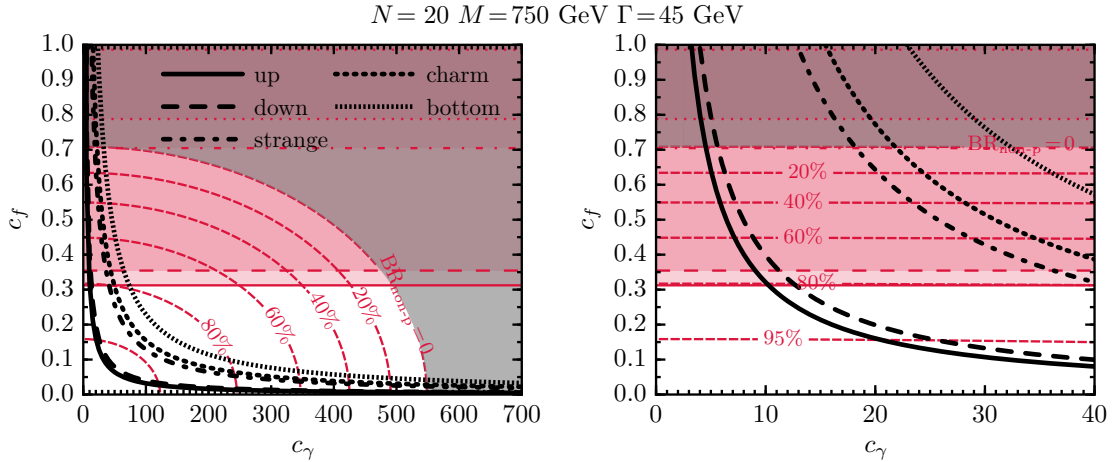


Figure 2. Points on black lines produce 20 signal diphoton events for a resonance with $M = 750$ GeV and $\Gamma = 45$ GeV. Different dashing indicates the various production modes, $u\bar{u}$, $d\bar{d}$, $s\bar{s}$, $c\bar{c}$, and $b\bar{b}$. Red dashed lines are contours of fixed $\Gamma_{\text{non-p}}$. The right panel is a blowup of the left one.

2.2 Interplay with previous LHC searches

Important additional information about the properties of the new particle can be obtained based on non-observation of any of its decays in Run 1 of the LHC, in particular in the 20 fb^{-1} of data collected at $\sqrt{s} = 8$ TeV.

First, let us consider limits from the diphoton resonance searches. For the broad

$i =$		gg	$q\bar{q}$	$t\bar{t}$	WW	ZZ	hh	Zh	$\tau\tau$	$Z\gamma$	$ee + \mu\mu$
$(\sigma_8 \times \text{BR}_i)^{\text{max}}$ [fb]		4000 [8]	1800 [8]	500 [9]	60 [10]	60 [11]	50 [12]	17 [13]	12 [14]	8 [15]	2.4 [16]
$p =$	gg	2600	1200	320	38	38	32	11	7.7	5.1	1.5
	$u\bar{u}$	1500	690	190	23	23	19	6.5	4.6	3.1	0.9
$\left(\frac{\text{BR}_i}{\text{BR}_{\gamma\gamma}}\right)^{\text{max}}$	$d\bar{d}$	1600	700	200	23	23	20	6.7	4.7	3.1	0.9
	$s\bar{s}$	2300	1000	280	34	34	28	9.6	6.8	4.5	1.4
	$c\bar{c}$	2400	1100	300	36	36	30	10	7.3	4.8	1.5
	$b\bar{b}$	2700	1200	340	40	40	34	11	8.1	5.4	1.6

Table 3. Top: Bounds on 750 GeV resonances from 8 TeV LHC searches. Bottom: Bounds on ratios of branching ratios for different production channel assumptions. For gg production, bounds on the branching fraction to $q\bar{q}$ are even tighter than indicated, since decays to gg will necessarily also be present and enter the dijet searches. The same applies to branching fraction to gg when the production is from quarks.

resonance hypothesis preferred by ATLAS, $\Gamma_S/M_S \approx 6\%$, most relevant is the CMS limit

$$\sigma_8 \times \text{BR}_{\gamma\gamma} \lesssim 2.5 \text{ fb}, \quad (2.12)$$

which was derived for scalar resonances with $\Gamma/M = 10\%$ [5]. For a narrow resonance, which might be preferred by the CMS data, the same search obtains the limit

$$\sigma_8 \times \text{BR}_{\gamma\gamma} \lesssim 1.3 \text{ fb}. \quad (2.13)$$

Somewhat weaker limits, of 2.5 and 2.0 fb respectively, were obtained by ATLAS [6] and CMS [7] for RS gravitons with $k = 0.1$, which are also narrow.

The compatibility of the observed excesses with the 8 TeV diphoton searches depends solely on the parton luminosity ratio, r_p , listed in Tab. 2. The ATLAS+CMS excess, Eq. (2.1), translates to

$$\sigma_8 \times \text{BR}_{\gamma\gamma} = \frac{\sigma_{13} \times \text{BR}_{\gamma\gamma}}{r_p} \approx \left(\frac{N}{20} \right) \times \{1.6, 2.6, 2.6, 1.8, 1.7, 1.5\} \text{ fb} \quad (2.14)$$

for the different production cases from Eq. (2.6). We see that $N = 20$ excess events at 13 TeV are borderline compatible with the 8 TeV analyses, especially if the resonance is broad. The gg and heavy-quark production modes are somewhat favoured in this respect because their luminosities increase more rapidly with \sqrt{s} .

The ATLAS and CMS collaborations performed searches for resonant signals in other final states as well. In Table 3 we list the various possible two-body final states relevant to a neutral spin-0 particle, and the corresponding 95% C.L. exclusion limits, $(\sigma_8 \times \text{BR}_i)^{\text{max}}$, from the 8 TeV searches. Searches for dijet resonances that employ b tagging, that would have enhanced sensitivity to $b\bar{b}$ final states, only address resonances heavier than 1 TeV [17, 18], but limits from $q\bar{q}$ searches still apply to $b\bar{b}$. Same for the recent 13 TeV dijet searches [19, 20]. We also note that the limits quoted in table 3 are approximate. In general, they do have some dependence on the width of the resonance, its spin, etc.

Table 3 also presents the resulting constraints on the ratios of branching ratios of the particle, for the different production channel assumptions. Those are computed as

$$\left(\frac{\text{BR}_i}{\text{BR}_{\gamma\gamma}} \right)^{\text{max}} = r_p \frac{(\sigma_8 \times \text{BR}_i)^{\text{max}}}{\sigma_{13} \times \text{BR}_{\gamma\gamma}} \quad (2.15)$$

where we use Eq. (2.1) and the parton luminosity ratios r_p from Table 2.

The dijet decay mode is always present since we expect the resonance to couple to either gg or $q\bar{q}$ for production. Also, the production cross section needs to be relatively large to accommodate the excess without too large c_γ , so limits on dijet resonances may restrict part of the parameter space of a concrete realisation. For the case in which a single production mode dominates we can obtain upper limits on c_p by saturating the gg or $q\bar{q}$ dijet bounds:

$$\begin{aligned} \text{BR}_p &< \sqrt{n_p \frac{M}{\Gamma} \frac{(\sigma_8 \times \text{BR}_p)^{\text{excl}}}{x_S^{8,p}}} \simeq \{25, 19, 25, 99, 124, 193\}\% \times \left(\frac{45 \text{ GeV}}{\Gamma} \right)^{1/2}, \\ |c_p| &< \{97, 0.31, 0.35, 0.70, 0.79, 0.99\} \times \left(\frac{\Gamma}{45 \text{ GeV}} \right)^{1/4}. \end{aligned} \quad (2.16)$$

By combining (2.16) with (2.9) and (2.4), we can obtain a second type of lower bound on $\text{BR}_{\gamma\gamma}$ and c_γ ,

$$\begin{aligned} \text{BR}_{\gamma\gamma} &> \{1.0, 2.9, 3.6, 9.7, 11, 16\} \times 10^{-4} \times \left(\frac{N}{20} \right) \left(\frac{5.8 \text{ fb}^{-1}}{\mathcal{L}_{13}} \right) \left(\frac{45 \text{ GeV}}{\Gamma} \right)^{1/2}, \\ |c_\gamma| &> \{5.5, 9.4, 11, 17, 19, 22\} \times \sqrt{\left(\frac{N}{20} \right) \left(\frac{5.8 \text{ fb}^{-1}}{\mathcal{L}_{13}} \right) \left(\frac{\Gamma}{45 \text{ GeV}} \right)^{1/4}}. \end{aligned} \quad (2.17)$$

In the $c_p - c_\gamma$ planes of Figs. 1 and 2, red areas are excluded by dijet searches. For illustration, we also show in the panels of Fig. 3 the relation between BR_p and $\text{BR}_{\text{non-p}}$. The black lines correspond to $N = 20$ signal events in the 13 TeV diphoton analyses. The left part of the plots correspond to the large c_γ solutions and the right to the small c_γ solutions. These plots also highlight the importance of $\text{BR}_{\text{non-p}}$, which in most of the viable parameter space is the dominant branching ratio. We show to what extent this width can be attributed to other decays into Standard Model particles.

3 Models

We now turn to concrete models.

3.1 Extra SM gauge singlet

The most general Lagrangian for an additional singlet up to dimension 5 terms is

$$\begin{aligned} \mathcal{L}_{\text{eff}} &= (\mu\Phi + \kappa\Phi^2)H^\dagger H \\ &+ \frac{\Phi}{f} \left(c_g^{\Phi} \frac{\alpha_s}{8\pi} G_{\mu\nu}G^{\mu\nu} + c_Y \frac{\alpha_1}{8\pi} B_{\mu\nu}B^{\mu\nu} + c_W \frac{\alpha_2}{8\pi} W_{\mu\nu}W^{\mu\nu} + c_{H1}|D_\mu H|^2 + c_{H2}|H|^4 \right) \\ &+ \frac{\Phi}{f} \left(Y_{ij}^d H \overline{Q_i} d_j + Y_{ij}^u \tilde{H} \overline{Q_j} u_d + Y_{ij}^e H \overline{L_i} e_j + h.c. \right). \end{aligned} \quad (3.1)$$

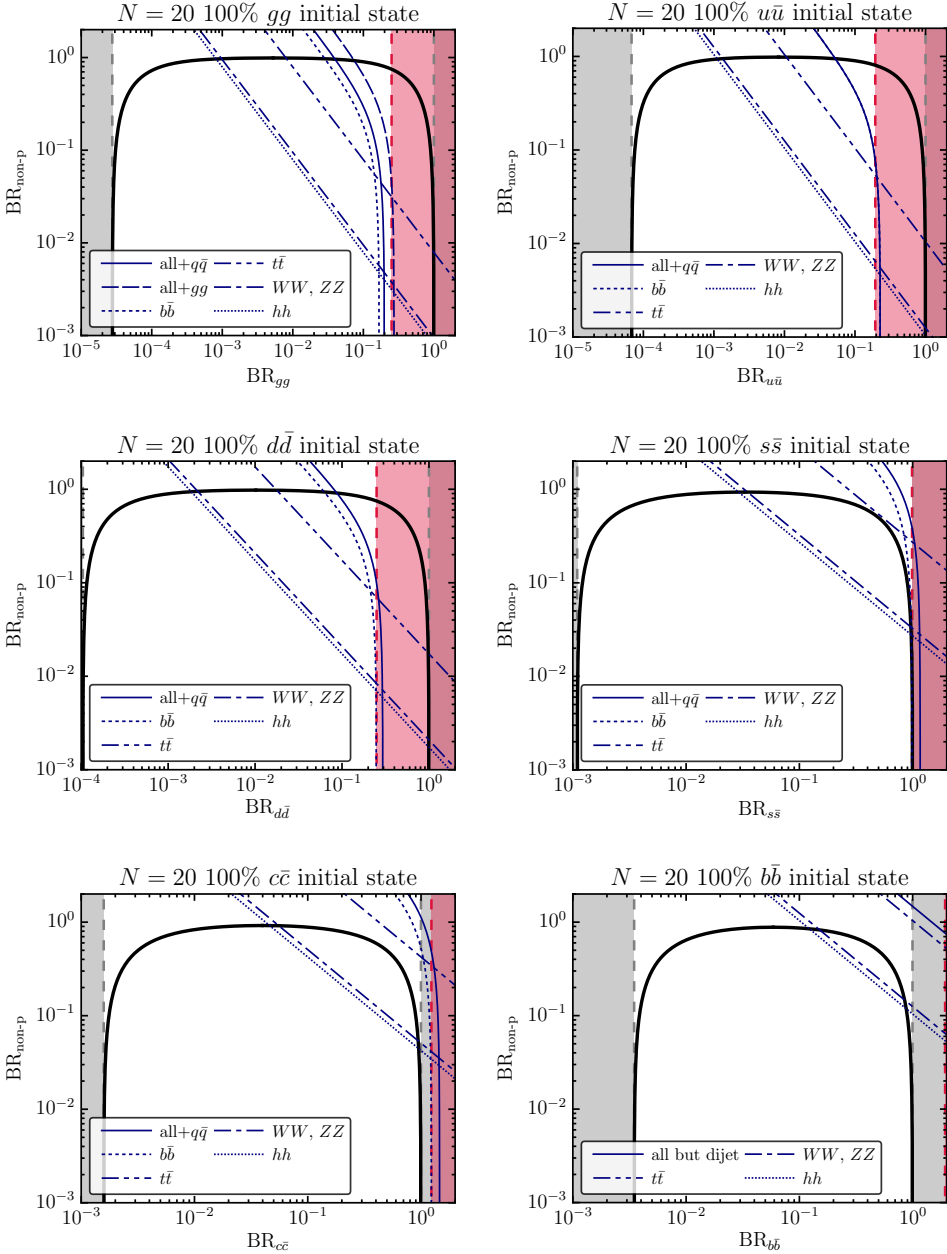


Figure 3. The plots, each for a different production mode, describe the condition to obtain $N = 20$ excess events, in terms of the branching fraction into the production mode (x axis) and that into modes other than production and diphoton (y axis). The condition is satisfied along the thick black lines. Grey regions are excluded by the requirement that the total width cannot be larger than the width of $\Gamma = 45$ GeV preferred by ATLAS. Red regions are excluded by 8 TeV dijet resonance searches. Thin lines described in the legend show the maximal branching fractions allowed by 8 TeV searches into final states from Tab. 3. The label ‘‘all’’ includes all the final states from the table except for gg and $q\bar{q}$.

The normalisation conventions agree with those of [21]. We will discuss two cases, first a renormalizable model where only the terms on the first line are present, and second, the dilaton of a spontaneously broken scale invariance, where the coefficients $c_{g,Y,W}^\Phi$ are present at the Lagrangian level, with coefficients related to the β -functions in the low-energy effective theory.

3.1.1 Renormalizable model with additional singlet

In the absence of the nonrenormalisable couplings, the κ term leads to a mixing with the SM CP even doublet component, and we obtain two mass eigenstates \mathcal{S} and the observed 125 GeV Higgs h . This results in \mathcal{S} having tree-level couplings proportional to those of the SM Higgs but suppressed by a universal factor,

$$g_i^{\mathcal{S}} = s_\alpha g_i^{h_{\text{SM}}}, \quad (3.2)$$

where $s_\alpha = \sin \alpha$, α being the mixing angle. Note that we must have $s_\alpha \lesssim 0.2$ to ensure that the total width of \mathcal{S} , which is dominated by the partial width to longitudinal electroweak gauge bosons, is less than 45 GeV. The coupling to the light quarks is thus negligible and thus production must be gluonic. At one-loop level, SM particles generate an effective c_g and c_γ . To get the largest possible c_g and c_γ we take $s_\alpha = 0.2$ and obtain,

$$c_g = 1.6, \quad c_\gamma = 0.09. \quad (3.3)$$

As we need $|c_g c_\gamma| \approx 530$, if we assume a 45 GeV resonance, this is far too small. Even if we allow for a smaller width we still cannot evade the bound in Eq. (2.11). Clearly we need either large loop contributions from new BSM states or a contribution from the irrelevant couplings in Eq. (3.1), in particular large values of c_g^Φ or the couplings to light quarks to enhance the production and large values of $c_{W,B}^\Phi$ to enhance the branching ratio. A large coupling of \mathcal{S} to light quarks is, however, problematic because in Eq. (3.1) in general the last term would lead to tree-level flavour changing neutral currents (FCNC) unless $f \gg v$ or the Y_{ij}^f are aligned to the SM Yukawa matrix. Thus we are led to find BSM contributions to boost c_g and c_γ .

3.1.2 Boosting c_g , c_γ with new vectorlike fermions

To investigate whether the exotic charged particles can generate large enough $c_{g,\gamma}$ we consider the minimal case of an additional vectorlike fermion charged under QCD having N_c colours and electromagnetic charge q , that couples to \mathcal{S} as follows,

$$\mathcal{L} = y_Q \mathcal{S} \bar{Q} Q - m_Q \bar{Q} Q. \quad (3.4)$$

The fermion loop will generate $c_{g,\gamma}$. A fermion with mass m_f , N_c colours, and Yukawa coupling y to a real scalar S contributes

$$c_g = g_s^2 y \tilde{A}_{1/2}^H(\tau_Q), \quad (3.5)$$

$$c_\gamma = 2N_c Q_f^2 e^2 y \tilde{A}_{1/2}^H(\tau_Q), \quad (3.6)$$

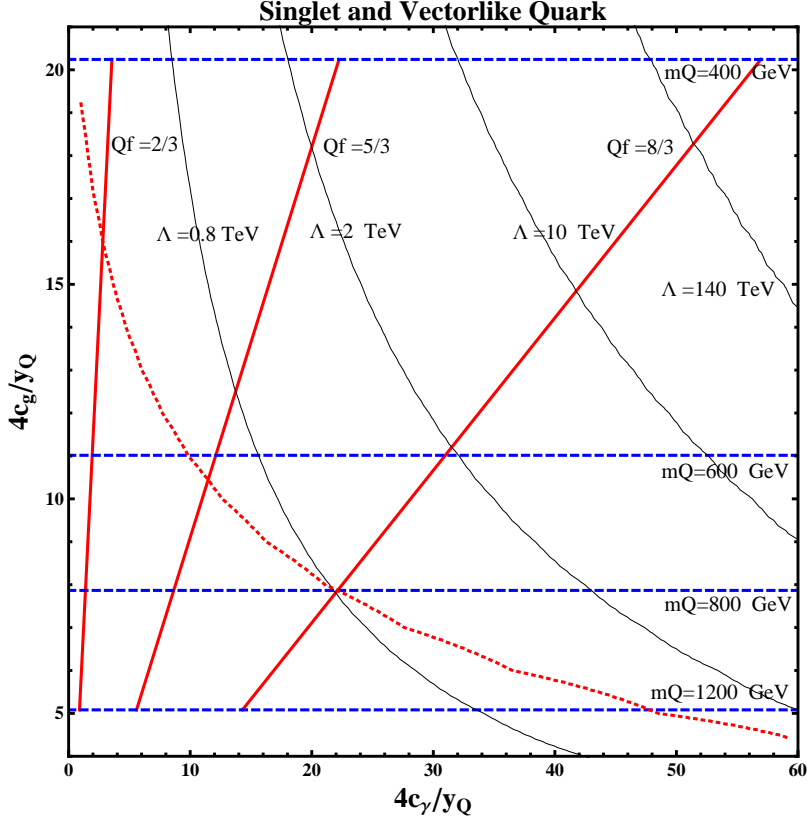


Figure 4. Contribution to the photonic and gluonic couplings c_γ and c_g of an SM singlet S due to vectorlike matter with charge Q_f and Yukawa coupling y_Q . Also shown are contours of the scale Λ at which the coupling y_Q becomes strong ($\mathcal{O}(4\pi/\sqrt{N_c})$), assuming we take it to be just large enough at each point in the c_g - c_γ plane to obtain $c_g c_\gamma = 530$) and explain the excess. For the region below the red dotted curve, the UV contribution from the cut-off (evaluated by assuming a fermion of same charge but with mass at the cut-off and $y_Q = 4\pi/\sqrt{N_c}$) is at least as large as the contribution from the fermion Q .

where $\tau_Q = M_S^2/(4m_f^2)$ and

$$\tilde{A}_{1/2}^H(\tau) = 2\tau^{1/2} A_{1/2}^H(\tau) = 4\tau^{-3/2}[\tau + (\tau - 1)f(\tau)] \quad (3.7)$$

with $f(\tau)$ defined in [22]. For $m_Q < m_S/2$ we get the constraint $y \lesssim 0.7$ by requiring that the total width is less than 45 GeV, which would lead to very small values of $c_{g,\gamma}$ and thus we take $m_Q > m_S/2$. In Fig. 4 we show the values of $c_{g,\gamma}$ generated as m_Q is varied between 400 GeV and 1.2 TeV assuming the total width of the resonance is 45 GeV. The values of $c_{g,\gamma}$ for $y_Q = 4$ can be directly read off from Fig. 1 and one can easily find the value for other y_Q values by keeping in mind that $c_{g,\gamma}$ scale linearly with y_Q . We can see that unless y_Q is large we cannot get $|c_g c_\gamma| \approx 530$, that is required to explain the excess. In some regions of the parameter space, this implies a low cut-off for the theory at the scale y_Q becomes strongly coupled. In Fig. 4 we also show contours of the scale Λ at which the coupling y_Q becomes strong ($\mathcal{O}(4\pi/\sqrt{N_c})$), assuming we take it to be just large enough at each point in the c_g - c_γ plane (to make $c_g c_\gamma = 530$) to explain the excess.

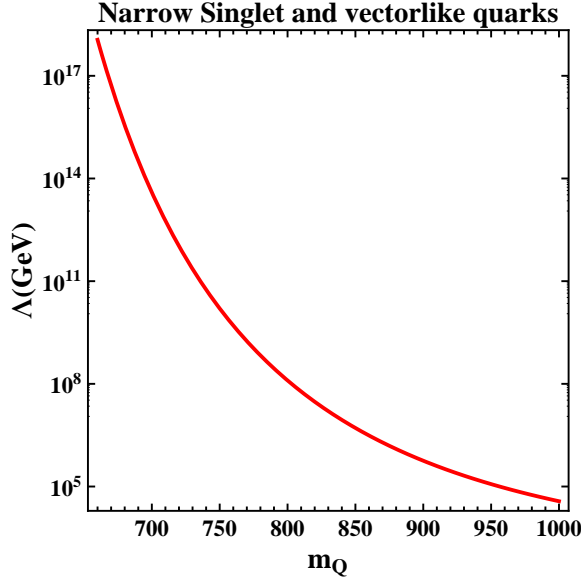


Figure 5. The scale of breakdown of perturbativity assuming we take the required y_Q to explain the excess, as a function of m_Q . For $m_Q < 660$ GeV the β function is negative so that the theory is completely perturbative in this region. The coupling y_Q varies from 2.6 to 4.1 for the range of m_Q shown.

We also mark the region (below the red dotted curve) where the UV contribution from the cut-off (evaluated by assuming a fermion of same charge but with mass at the cut-off and $y_Q = 4\pi/\sqrt{N_c}$) is as large as the contribution from Q . It is clear that the theory becomes strongly coupled below 2 TeV unless we take a large value for the electric charge ($Q_f = 8/3$). For a large charge the negative contribution to the running proportional to $y_Q g'^2$, can actually push the cut-off to values as high as 100 TeV, as one can see from the top right of Fig. 4. Note that we cannot push the strong coupling scale higher by taking a large number, N_f , of flavors or larger QCD representations and thus a smaller y_Q , as there are terms proportional to $N_f y_Q^2$ and $N_c y_Q^2$ that appear in the RGE for y_Q . In a complete theory there must be additional interactions that allow these vectorlike quarks to decay via mixing to SM quarks. Note that in most of the parameter space a large invisible width (greater than 35 GeV) needs to be assumed in most of the parameter space if we assume a 45 GeV width for the resonance. Also, the dijet constraint $c_g \lesssim 125$ is satisfied in the full parameter space even after rescaling y_Q appropriately to explain the signal.

If we do not assume any invisible width and allow the resonance to have a narrow width the total width would be dominated by $\Gamma(S \rightarrow gg)$ as $\Gamma(S \rightarrow gg) \gg \Gamma(S \rightarrow \gamma\gamma)$ for $\mathcal{O}(1)$ charges (see Eq. (3.6)). We then only need a $c_\gamma \gtrsim 2.5$ in accordance with Eq. (2.11). In Fig. 5 we show the scale of breakdown of perturbativity assuming the required y_Q to obtain $c_\gamma \gtrsim 2.5$, as a function of m_Q . We see that the theory is perturbative up to very large scales.

We, thus find that that for a 45 GeV singlet resonance the size of the excess might

hint to strongly coupled physics at a few TeV unless there are fermions around or below the mass of the resonance with large electric charge. If we allow for a narrow width we still require additional charged states but the theory can be totally perturbative. The hints of strongly coupled physics motivate us to examine in more detail a popular strongly coupled scalar candidate, the dilaton.

3.2 The dilaton

The couplings of the dilaton in the EW broken phase are given by [21],

$$\mathcal{L}^{dil} = \frac{\Phi}{f} \left(\sum_f m_f \bar{f} f + 2 \sum_f (m_W^2 W^+ W^- + \frac{m_Z^2}{2} Z^2) + \frac{c_g^\Phi \alpha_s}{8\pi} G_{\mu\nu} G^{\mu\nu} + \frac{c_\gamma^\Phi \alpha_{EM}}{8\pi} F_{\mu\nu} F^{\mu\nu} \right) \quad (3.8)$$

Furthermore, in general, there will be a mixing term with the SM Higgs, that can arise from either the term $\Phi H^\dagger H$ in the potential or kinetic mixing [23], so that finally we obtain two mass eigenstates \mathcal{S} and the observed 125 GeV Higgs h where,

$$\mathcal{S} = s_\alpha h_{\text{SM}} + c_\alpha \Phi. \quad (3.9)$$

where we expect $s_\alpha = \mathcal{O}(v/f)$. Thus we get for the coupling to fermions and gauge bosons,

$$\begin{aligned} g_{V,f}^{\mathcal{S}} &= \xi g_{V,f}^{h_{\text{SM}}} \\ \xi &= s_\alpha + \frac{v}{f} c_\alpha \end{aligned} \quad (3.10)$$

As in the case of the renormalizable singlet model, unless $\xi \lesssim 0.2$, the total width will exceed 45 GeV. As the sign of s_α is arbitrary and $s_\alpha = \mathcal{O}(v/f)$ we expect $\xi = \mathcal{O}(v/f)$. This constrains,

$$f \gtrsim 1.2 \text{ TeV}. \quad (3.11)$$

For the dilaton, the couplings $c_{g,\gamma}^\Phi$ can be completely determined using the low energy theorems and scale invariance [21]. We obtain for the dilaton coupling to gluons,

$$\frac{\sum_{\text{heavy}} b_0^i \alpha_s}{8\pi} G_{\mu\nu} G^{\mu\nu} \quad (3.12)$$

where b_0^i is the contribution of the field i to the QCD β -function,

$$\beta_i = \frac{b_0^i g_s^3}{16\pi^2} \quad (3.13)$$

and the sum is over all particle heavier than the scale f . Scale invariance implies,

$$\sum_{\text{heavy}} b_0^i + \sum_{\text{light}} b_0^i = 0. \quad (3.14)$$

so that we finally get,

$$c_g^\Phi = - \sum_{\text{light}} b_0^i. \quad (3.15)$$

For a dilaton heavier than the top quark (as the case must be here) and assuming that the full SM is part of the conformal sector we must sum over all SM coloured states which gives $\sum_{\text{light}} b_0^i = -7$. Note that if we do not include all SM fields in the conformal/composite sector [24] and keep some SM fields elementary that explicitly break scale invariance, $\sum_{\text{light}} b_0^i$ would decrease. Similarly one obtains [21],

$$c_\gamma^\Phi = -11/3. \quad (3.16)$$

For $f = 1.2$ TeV we obtain,

$$c_g = 13.9, \quad c_\gamma = 0.48. \quad (3.17)$$

where we have again assumed $s_\alpha = \mathcal{O}(v/f)$. Again we find $c_g c_\gamma \ll 500$ and is thus inadequate to explain the excess. We see to explain the excess we need large additional contributions to the QCD and QED β functions below the scale f ,

$$\begin{aligned} \Delta c_g &= \frac{2g_s^2 \Delta b_{\text{QCD}} m_s}{f} \\ \Delta c_\gamma &= \frac{2e^2 \Delta b_{\text{QED}} m_s}{f} \end{aligned} \quad (3.18)$$

For n_f additional vectorlike colour-triplet, SU(2)-singlet fermions we have,

$$\begin{aligned} \Delta b_{\text{QED}} &= \frac{4N_c n_f}{3} Q_f^2 \\ \Delta b_{\text{QCD}} &= \frac{2}{3} n_f \end{aligned} \quad (3.19)$$

where Q_f^2 is the electric charge of the fermion. Clearly to enhance c_g or c_γ to a magnitude such that $c_g c_\gamma \approx 530$ as required by the data to explain the excess, we need either an unusually large charge Q or a very large number of flavours n_f of additional fermions below the TeV scale. This scenario thus does not seem feasible

Note that for the dilaton, allowing a smaller width would actually decrease the signal. This is because the narrow width would require a large f which would decrease the production but keep the branching ratio to photons unchanged.

Note that even if it is possible to boost c_g or c_γ in some variant of the above set up, dilaton and radion models would in general be strongly constrained by 8 TeV diboson searches. Using the constraint from Table 3 this constraint would imply,

$$\frac{\text{BR}(\mathcal{S} \rightarrow WW)}{\text{BR}(\mathcal{S} \rightarrow \gamma\gamma)} \gtrsim 46. \quad (3.20)$$

For the numbers in Eq. (3.17), the right hand side above is $\mathcal{O}(10^4)$.

3.3 Additional Pseudoscalar

We now consider the case of an additional pseudoscalar. It can appear in composite models as a Pseudo Nambu Goldstone Boson (PNGB) [25]. Unlike the scalar it cannot mix with the SM Higgs and some couplings like those to longitudinal W s and Z in Eq. (3.1) are

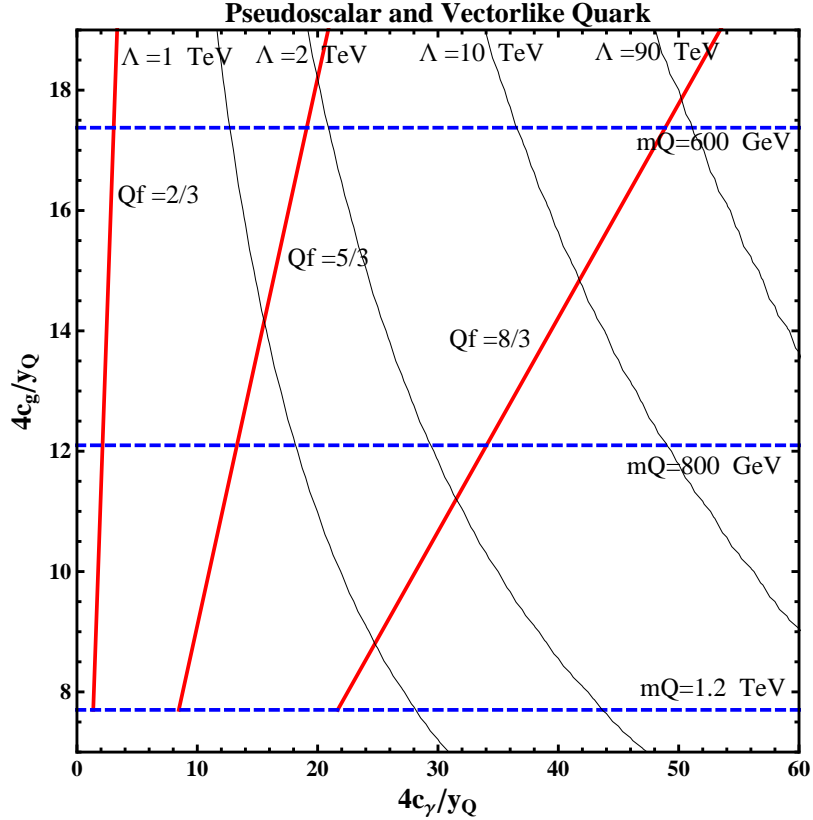


Figure 6. Contribution to the photonic and gluonic couplings c_γ and c_g of a pseudo scalar due to vectorlike matter with charge Q_f and Yukawa coupling y_Q . In grey are contours of the scale Λ at which the coupling y_Q becomes strong ($\mathcal{O}(4\pi/\sqrt{N_c})$), where we have fixed $y_Q(M_S)$ by requiring the correct signal size.

not allowed. This is therefore an example, where unlike the dilaton, the ratio of the partial width to electroweak bosons and photons is not expected to be very large and is thus it is not so severely constrained by diboson searches. The most general terms are,

$$\begin{aligned} \mathcal{L} &= -\frac{1}{16\pi^2} \frac{1}{4} \frac{c_B}{M_S} \mathcal{S} B^{\mu\nu} \tilde{B}_{\mu\nu} - \frac{1}{16\pi^2} \frac{1}{4} \frac{c_W}{M_S} \mathcal{S} W^{a\mu\nu} \tilde{W}_{\mu\nu}^a - \frac{1}{16\pi^2} \frac{1}{4} \frac{c_g}{M_S} \mathcal{S} G^{\mu\nu,a} \tilde{G}_{\mu\nu}^a + y_Q \mathcal{S} \bar{Q} \gamma_5 Q \\ &\Rightarrow -\frac{1}{16\pi^2} \frac{1}{4} \frac{c_\gamma}{M_S} \mathcal{S} F^{\mu\nu} \tilde{F}_{\mu\nu} - \frac{1}{16\pi^2} \frac{1}{4} \frac{c_g}{M_S} \mathcal{S} G^{\mu\nu,a} \tilde{G}_{\mu\nu}^a + y_Q \mathcal{S} \bar{Q} \gamma_5 Q. \end{aligned} \quad (3.21)$$

where we have also included a coupling to a vectorlike quark. Following the same procedure as in Sec. 3.1.2 we show the contribution of the vectorlike quark loop to c_g and c_γ in Fig. 6 and the scale where y_Q becomes non-perturbative.

3.4 Excluding the general 2HDM

In this part we discuss the possibility where the excess can be explained within the framework of general two Higgs doublet model (2HDM). Our starting point is the decoupling limit, as we are interested in the case where we have new spin zero states at a mass scale $M \approx 750$ GeV, that is considerably larger than the weak scale. We can thus think of the

ratio $\epsilon \equiv v/M \ll 1$ as our formal expansion parameter (see [26] and Refs. therein for relevant discussions). In this limit it is useful to describe the theory in the so called Higgs basis [27], where only one of the two doublets, that corresponds to the SM Higgs, acquires a VEV. In more detail the mass eigenstates are contained in a light SM-like Higgs doublet, H_a , with VEV equal to 246 GeV and a heavy (degenerate to a good accuracy) doublet, H_b , consisting of four additional spin zero degrees of freedom with a vanishing VEV. For simplicity we work in the CP conserving limit. The misalignment between the Higgs basis and the mass basis is of order ϵ .

An important comment is in order here: When one matches this expansion parameter to the actual 2HDM potential in the decoupling limit, the corrections to various couplings would be typically of order of $\lambda \times \epsilon^2$ with λ stands for some quartic parameter. As we are interested in this part in a perturbative explanation for the resonance we assume in general $\lambda \lesssim 1$. Therefore $\epsilon^2 \sim 0.1$ can serve as a useful formal expansion parameter. We note however that when we exclude the pure 2HDM case, in the following section, we in fact allow values of λ that are much bigger than unity which makes it robust.

One interesting consequence of the decoupling limit is that the splitting in the mass square between the neutral CP even state H^0 and odd one A is of the order of ϵ^2 and thus generically small,

$$\delta m = |m_{H^0} - m_A| \lesssim \epsilon^2 \times \frac{M}{2} \sim 45 \text{ GeV}. \quad (3.22)$$

As δm is compatible with the extracted width of the excess, we conclude that it is quite possible that actually the observed signal might arise due to the presence of these two neighbouring states.

3.4.1 Excluding the Pure 2HDM case

In this part we show that in the decoupling limit, and assuming no additional states, beyond the additional doublet and allowing for only relevant and marginal couplings to be present, the generic 2HDM cannot account for the observed excess. We note that in this limit the couplings of the heavy states to the light quarks can differ significantly from that of the SM Higgs-couplings, as was exploited in [28]. In particular the couplings of H_b to the light quarks might be compatible with the ones extracted in the model independent part (see Eq. (2.10)). Thus, in this part we consider production through either quark-anti-quark or gluon fusion. In addition as the signal can be generically accounted for by the presence of both H^0 and A we should consider the production and decay of each of these. We emphasise that to be conservative we do not require the width to be equal to 45 GeV as the excess could be explained by the two narrower states separated in mass by few tens of GeV, which would be consistent with the published di-photon spectrum. We denote N_H as the number of events produced from the production and decay of H^0 , in the CP limit we can assume no interference between the different two production modes.

As explained in the above, given a number of signal event, one can derive a lower bound on the value of c_γ (which is independent of the width, and as long as the BR into photons is subdominant). This bound depend on the production mechanism and we derive it separately for the glue-glue and $q - \bar{q}$ production modes.

Glue-glue production: Assuming that the masses of A and H^0 are less than 45 GeV apart, both states would contribute to the excess. To obtain this bound, first of all, note that for the total width of the resonance not to exceed 45 GeV we must have,

$$\sum_f y_f^2 < 0.44, \quad (3.23)$$

y_f being the coupling of H^0 and A to the SM fermions. As the production and decay of the resonances are thorough fermion loops and as the fermionic loop contribution decreases with the mass of the fermion to maximise the number of events we must allow $y_t = 0.66$ and saturate the above bound.

We first bound the pseudo-scalar induced contributions. We notice that in the CP limit, its couplings to the photons and gluons is only due to presence of fermions in the loop. The total number of events from pseudo scalar decay events can be derived from Eq. (2.4),

$$N_A = 4.0 \times 10^5 \times \text{BR}_{\gamma\gamma} \times \frac{\Gamma(A \rightarrow GG)}{\Gamma(A)} \times \frac{\Gamma(A)}{45 \text{ GeV}} < 4.0 \times 10^5 \times \frac{\Gamma(A \rightarrow GG) \times \Gamma(A \rightarrow \gamma\gamma)}{\Gamma(A \rightarrow ff)^2}, \quad (3.24)$$

where,

$$\begin{aligned} \Gamma(A \rightarrow gg) &= \frac{y_t^2 \alpha_s^2}{32\pi^3 m_t^2} m_A^3 \left| \sum_f A_f^A \right|^2 \\ \Gamma(A \rightarrow \gamma\gamma) &= \frac{y_t^2 \alpha^2 m_A^3}{64\pi^3 m_t^2} \left| \sum_f N_c Q_f^2 A_f^A \right|^2, \end{aligned} \quad (3.25)$$

and $\Gamma(A \rightarrow ff) = 0.11 M y_t^2$ from table 1. Taking $y_t = 0.67$ one can now evaluate the upper bound in Eq. (3.24),

$$N_A < 0.005. \quad (3.26)$$

We thus conclude that the pseudo scalar contributions are negligibly small in this case.

Next we consider the contribution from H^0 production. To explain the signal we thus require that all 20 signal events must be via H decay,

$$20 = N_H < 1.0 \times 10^4 \times \frac{\Gamma(H \rightarrow GG)(y_t)}{\Gamma(H \rightarrow tt)(y_t)} \times \Gamma(H \rightarrow \gamma\gamma)(c_\gamma) \text{ GeV}^{-1}, \quad (3.27)$$

where as in the above we have used the maximal value of the coupling of H_A to the top quark in order to maximise the ratio $\frac{\Gamma(H \rightarrow GG)(y_t)}{\Gamma(H \rightarrow tt)(y_t)}$ which is then becoming independent of y_t . This gives us,

$$c_\gamma > 65. \quad (3.28)$$

The real scalar contributions arise both due to fermionic loops and loops include the charged electroweak vector bosons and heavy Higgs bosons. We note that the contributions related to the heavy charged Higgs effect the total width of H^0 only at subleading order due to there large mass. In order to check whether general 2HDM can account for such a value

of c_γ we have added up the loop contributions from the top quark the W and the charged Higgs (see e.g. [22]). We find that over the entire relevant parameter space c_γ cannot be bigger than 5. Therefore, we conclude that production due to gluon fusion processes cannot account for the observed anomaly.

Fermion-fermion production: As argued above in general the heavy states can have sizable contributions to the first two generation. Ignoring possible severe constraints from flavor physics we find that the weakest bound is due to $\bar{u}u$ production. Using Eq. (2.11) it gives

$$c_\gamma > 4.1. \quad (3.29)$$

In the Higgs basis the only two operators that could induce such a big couplings are related to the term $\lambda_{H+}(H_A^\dagger H_B)(H_B^\dagger H_B) + \lambda_{W+}(H_B^\dagger H_A)(H_A^\dagger H_A)$. Where the term proportional to λ_{H+} (λ_{W+}) generates the charged-higgs (W) loop induce contributions. The constraint from the width implies that $\lambda_{W+} < 0.2$ and hence it contributes to c_γ only in a negligible way. The contributions to c_γ proportional to λ_{H+} are unconstrained by the width and can be significantly larger. However we find that even if we take λ_{H+} to its formal perturbative limit, namely $16\pi^2$ and even in this case we get only c_γ as large as 3 which yield only half of the required number of events. In any case this violates our assumption of perturbativity as with this coupling the theory is strongly coupled at the scale 750 GeV.

Last remain the contribution to the CP odd scalar from $u\bar{u}$ that is dominates by the loop contribution with internal top. We have verified that it yields a negligible contribution and by this we have verified that the general 2HDM model cannot account for the observed anomaly.

3.5 The fate of the MSSM

We now turn to the Minimal Supersymmetric Standard Model (MSSM). As in the 2HDM, which in its model-II form is contained in the MSSM as a subsector, the only candidate particles for the resonance in the MSSM are H and A . Again, the only viable production mode is from gluon fusion, due to small Yukawa couplings and the fact that we are deep in the decoupling regime, $M_H \gg M_Z$. As we have seen above, the 2HDM fails by a large margin to accommodate the data. However, in the MSSM there are extra contributions to the Hgg couplings from sfermions and to the $H\gamma\gamma$ couplings from sfermions and charginos, in addition to those already present in the 2HDM. The Agg and $A\gamma\gamma$ vertices receive no sfermion contributions at one loop as a consequence of CP symmetry, though they do receive contributions from charginos.² Dimensional analysis gives, for the contribution of the two stops, for $M_{\text{SUSY}} = 1$ TeV,

$$c_g \sim 2g_s^2 \times \frac{M_H^2}{M_{\text{SUSY}}^2} \sim 2.2$$

²As in the rest of this work, we assume CP conservation. Without this assumption, some superposition of the two heavier mass eigenstates H_2 and H_3 will receive squark loop corrections, so apart from a division of the diphoton signal between H_2 and H_3 resonant contributions, we do not expect qualitative changes to our conclusions.

and

$$c_\gamma \sim 2N_c e^2 \times \frac{M_H^2}{M_{\text{SUSY}}^2} \sim 0.44.$$

This suggests that generically, the product $|c_g \times c_\gamma| \sim 1$, is nearly three orders of magnitude below what is required according to Eq. (2.9). However, the theoretical prediction scales quadratically with the loop contribution, and we must also contemplate that the true resonance width could be less than the “nominal” 45 GeV. The decay width of H is dominated by tree-level decays into top and bottom quarks, and is essentially determined in the MSSM as a function of $\tan \beta$, with a minimum of about 2 GeV at $\tan \beta \approx 6$. Hence, Eq. (2.9) can be recast as

$$\frac{|c_\gamma c_g|}{\sqrt{\Gamma(\tan \beta)/(45 \text{ GeV})}} = \rho_g \approx 530. \quad (3.30)$$

The question is how large the left-hand side may be. First, a small numerator could be partly compensated for by a factor of up to five due to the denominator. Second, an MSSM spectrum could also be quite non-degenerate, with hierarchies like $m_{\tilde{t}_1} \ll M_H, \mu \ll m_{\tilde{t}_2}$; this is in fact favoured by the observed Higgs mass. In particular, large μ and/or A -terms and a light stop can lead to a parametric enhancement $\sim \{\mu, A_t\}/m_{\tilde{t}_1}$. Third, there could also be important contributions from sbottoms and staus, as well as charginos, which brings in a large subset of the MSSM parameters. A conclusion about the fate of the MSSM requires a quantitative treatment, but a brute-force parameter scan is not really feasible and in any case beyond the scope of this work. Instead, the purpose of the rest of this section is to obtain simple yet conservative bounds on all one-loop contributions over the entire MSSM parameter space. The key assumption will be the absence of charge- and colour-breaking minima of the scalar potential. This could in principle be relaxed to only require metastability over cosmological timescales; we leave this aside for future work. The only other assumption we will be making is $\tan \beta > 1$, a violation of which would lead to a Landau pole in y_t , and/or strong coupling at low scales, and has very strong support from the observed Higgs mass of 125 GeV (which we will not separately impose). As we will see, these rather minimal assumptions are sufficient to exclude the MSSM if the resonance interpretation is confirmed.

3.5.1 Constraints from vacuum stability

An essential role in our argument is played by the upper bounds on the μ -parameter and the soft trilinear terms that follow from requiring the absence of charge- and colour-breaking minima of the MSSM scalar potential. The derivation of these bounds is well known [29–36] and involves suitable one-dimensional directions of the MSSM scalar field space. Employing the four directions

$$T_L = T_R = H_u^0, \quad B_L = B_R = H_d^0, \quad B_L = T_R = H_d^-, \quad T_L = B_R = H_u^+ \quad (3.31)$$

(with all other scalar fields held at zero), of which the first two are D -flat, the bounds following from the four can be conveniently formulated in terms of the stop and sbottom

masses, as follows:

$$|A_t| \leq \sqrt{3} \sqrt{m_{\tilde{t}_1}^2 + m_{\tilde{t}_2}^2 - 2m_t^2 + \frac{M_H^2}{2} [1 + \cos(2\beta)] - \frac{M_Z^2}{2} \cos(2\beta)}, \quad (3.32)$$

$$|A_b| \leq \sqrt{3} \sqrt{m_{\tilde{b}_1}^2 + m_{\tilde{b}_2}^2 - 2m_b^2 + \frac{M_H^2}{2} [1 - \cos(2\beta)]}, \quad (3.33)$$

$$|\mu| \leq \sqrt{1 + \frac{m_Z^2}{m_t^2} \sin^2 \beta} \quad (3.34)$$

$$\begin{aligned} m_b |\mu| \tan \beta &\leq m_t \sqrt{\frac{\tan^2 \beta}{R^2} + \frac{m_Z^2}{m_t^2} \sin^2 \beta} \\ &\quad \times \sqrt{m_{\tilde{b}_1}^2 + m_{\tilde{b}_2}^2 - 2m_b^2 + \frac{M_H^2}{2} [1 + \cos(2\beta)] + \frac{M_Z^2}{2} \cos(2\beta)}, \end{aligned} \quad (3.35)$$

where $R = m_t/m_b \sim 50$. The second and fourth bounds hold, upon substituting $b \rightarrow \tau$, for the stau sector, as well. No simplifications have been made. The first bound (rarely) has no solution; this means that the corresponding very light stop mass values are excluded on theoretical grounds. We can combine the bounds into bounding functions Φ_t , Φ_b , and Φ_τ of the sfermion masses and β only. Firstly,

$$\Phi_t = \begin{cases} 0, & m_{\tilde{t}_1}^2 + m_{\tilde{t}_2}^2 - 2m_t^2 + \frac{M_H^2}{2} [1 + \cos(2\beta)] - \frac{M_Z^2}{2} \cos(2\beta) < 0, \\ \sqrt{3} \sqrt{m_{\tilde{t}_1}^2 + m_{\tilde{t}_2}^2 - 2m_t^2 + \frac{M_H^2}{2} [1 - \cos(2\beta)] - M_Z^2 \cos(2\beta)}, & \text{otherwise.} \end{cases} \quad (3.36)$$

(If the condition for $\Phi_t = 0$ is satisfied, there is no way to satisfy the A_t constraint; setting the bounding function to zero in this case will serve to effectively discard those unphysical points below.) Otherwise, Φ_t simultaneously bounds both $|A_t|$ and $|\mu|$. A similar function that simultaneously bounds $|A_b|$ and $\frac{m_b}{m_t} |\mu| \tan \beta$ is provided by

$$\Phi_b = \sqrt{3} \sqrt{m_{\tilde{b}_1}^2 + m_{\tilde{b}_2}^2 - 2m_b^2 + \frac{M_H^2}{2} [1 - \cos(2\beta)]}, \quad (3.37)$$

and an identical function Φ_τ follows from this upon substituting $b \rightarrow \tau$.

3.5.2 Conservative bounds on sfermion contributions

In the notation of [37], the sfermion contributions to c_g is given by

$$\left| \sum_f c_g^{(\tilde{f})} \right| = \frac{g M_H}{2 M_W} g_s^2 \left| A_{\text{SUSY}, \tilde{f}}^H \right|. \quad (3.38)$$

If the contribution of a sfermion to c_g is known, the corresponding contribution to c_γ is given by

$$c_\gamma^{(\tilde{f})} = 2(e^2/g_s^2) N_c^{(f)} Q_f^2 c_g^{(\tilde{f})}. \quad (3.39)$$

Explicitly,

$$A_{\text{SUSY},\tilde{f}}^H = 4 \sum_{\tilde{f}=\tilde{t},\tilde{b},\tilde{\tau}} \sum_{i=1,2} \frac{g_{\tilde{f}_i \tilde{f}_i}^H}{M_H^2} h(\tau_i^q) \quad (3.40)$$

where $\tau_i^f = M_H^2/(4m_{\tilde{f}_i}^2)$ and

$$h(\tau) = \tau A_0^H(\tau) = \begin{cases} \frac{\arcsin^2(\sqrt{\tau})}{\tau} - 1 & \tau \leq 1, \\ -\frac{1}{4\tau} \left(\ln \frac{1+\sqrt{1-\frac{1}{\tau}}}{1-\sqrt{1-\frac{1}{\tau}}} - i\pi \right)^2 - 1 & \tau > 1. \end{cases} \quad (3.41)$$

Consider first the stops. In the decoupling limit, their couplings to H are

$$g_{\tilde{t}_i \tilde{t}_i}^H = -\cot \beta m_t^2 + x \sin(2\beta) M_Z^2 \pm m_t \frac{\sin(2\theta_t)}{2} (\mu + A_t \cot \beta), \quad (3.42)$$

where θ_t is the stop mixing angle, x and y depend on θ_t and β and are always less than one in magnitude. Using that $h \rightarrow 0$ for $\tau \rightarrow 0, \infty$ and $|h| \leq h(1) \approx 1.47$, one easily shows that the first two terms lead to maximal contributions to $A_{\text{SUSY},\tilde{t}}^H$ that are bounded (in magnitude) by $2.74 \cot \beta$ and 0.03 , respectively. (Similar terms for the sbottom and stau cases will be negligible.) The third term in the coupling leads to

$$A_{\text{SUSY},\tilde{t}}^H = \frac{\sin(2\theta_t)}{2} \frac{4 m_t (A_t \cot \beta + \mu)}{M_H^2} \times (h(\tau_1) - h(\tau_2)). \quad (3.43)$$

Employing now the bounding function Φ_t from the previous subsection, it is not difficult to show that

$$\left| m_t \frac{\sin(2\theta_t)}{2} (A_t \cot \beta + \mu) \right| \leq m_t \min \left(\frac{1}{2} \Phi_t(1 + \cot \beta), m_t \frac{\Phi_t^2}{m_{\tilde{t}_2}^2 - m_{\tilde{t}_1}^2} \right) \equiv \frac{m_H^2}{4} B(\tau_1, \tau_2; M_H). \quad (3.44)$$

The first argument of the min function follows from $|\sin| \leq 1$, the second makes use of the explicit formula for the stop mixing angle. We then have

$$|A_{\tilde{t}}^H| \leq B(\tau_1, \tau_2) |h(\tau_1) - h(\tau_2)|. \quad (3.45)$$

The right-hand side is bounded and the physical parameter space is the compact region $0 \leq \tau_i \leq \tau_i^{\max}$, where $\tau_i^{\max} = M_H^2/(4m_{\tilde{m}}^{\min})$ depends on the experimental lower bound on the lighter stop mass. Straightforward numerical techniques establish that

$$|A_{\tilde{t}}^H| \leq 3.37, \quad (3.46)$$

where the maximum is obtained at $\tan \beta = 1$, when one stop is at threshold ($m = M_H/2$) and the other is relatively light. Below, we numerically obtain and use the bounds as a function of $\tan \beta$. (We allow stop masses as light as 100 GeV in the scan, to escape any doubts related to for instance compressed spectra where light stops might have escaped detection at the LHC). The extremal point is generally ruled out by the observed Higgs

mas $m_h = 125$ GeV, and very unlikely to be consistent with LHC searches, but we are being conservative.

Analogous steps lead to bounds on the sbottom and stau contributions. In this case, terms proportional to $m_{b,\tau}^2$ and m_Z^2 in the Higgs-sfermion couplings lead to completely negligible effects. For the remainder, we require a bound

$$\begin{aligned} \left| m_b \frac{\sin(2\theta_b)}{2} (\mu - A_b \tan \beta) \right| &\leq m_t \min \left(\frac{1}{2} M_b \left[\cot \beta + \frac{\tan \beta}{R} \right], \right. \\ &\quad \left. m_t \frac{M_b^2}{m_{\tilde{b}_2}^2 - m_{\tilde{b}_1}^2} \left[\cot \beta + \frac{\tan \beta}{R} \right] \left[1 + \frac{1}{R} \right] \right) \\ &\equiv \frac{m_H^2}{4} B_{\tilde{b}}(\tau_1, \tau_2; M_H). \end{aligned} \quad (3.47)$$

The resulting bound is most effective in the intermediate- $\tan \beta$ region, counteracting the small denominator of Eq. (3.30) in that region. The bound on the stau contribution, as a function of $\tan \beta$ and the slepton masses, is identical to the sbottom one, except for a missing colour factor (overcompensated in the photonic coupling by a ninefold-larger electric charge).

3.5.3 Contributions from other particles and verdict

The contributions from top and bottom loops have already been discussed in the 2HDM section. Regarding charginos, their effect is equivalent to the contribution of two vector-like, colourless particles; such contributions have also been discussed above. We only need to bound the fermion loop function by its global maximum and make no use of the relation of the chargino and Higgs mixing angles in order to obtain the bound $|\alpha_\gamma^{X^+}| \leq 0.45$ (for any $\tan \beta$). Assuming now the extreme scenario where all contributions to c_γ and c_g simultaneously saturate their bounds and are in phase with one another, we obtain a (very) conservative upper bound on the left-hand side of Eq. (3.30). This is displayed in Figure 7. We observe that this bound still misses the data by more than a factor of two, even at the point of closest approach at $\tan \beta \sim 4$. It is fairly clear that the bound could be made stronger by, for example, employing more properties of the function h or formulating a higher-dimensional extremization problem (closer to a full scan of the MSSM parameter space). We must also stress that our conclusions here are specific to the MSSM, and attest to the high predictivity of the model. If the MSSM cannot survive in regions of metastability (where charge and colour-breaking minima exist but are not tunneled to over cosmological timescales, an unlikely possibility), more complicated supersymmetric models might hence still accommodate the excess, although the techniques described here may be useful in scrutinizing them. Another logical possibility of saving the MSSM would be production through the decay of a heavier particles (say, stops, which could themselves be produced from gluino and squark decays). As mentioned in the beginning, there experimental data does not seem to support such a mechanism.

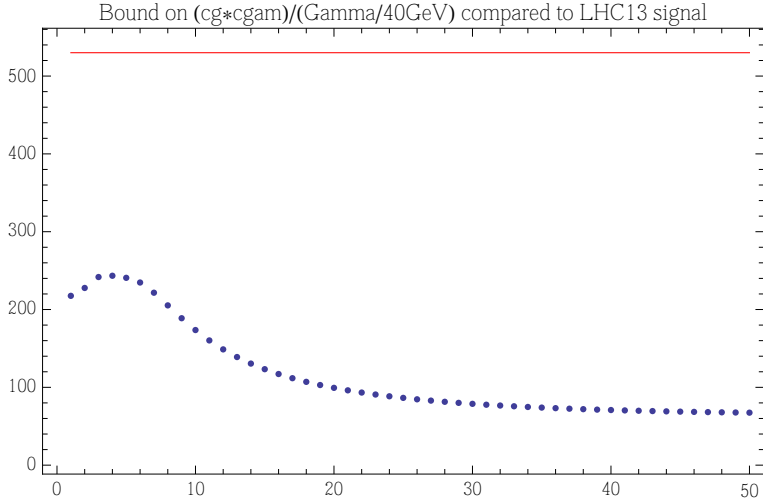


Figure 7. Comparison of the upper bound in Eq. (3.30) to the signal suggested by the diphoton excesses, as a function of $\tan \beta$ (horizontal axis). The red horizontal line corresponds to the signal, the blue dots represent our conservative upper bound.

4 Summary and Outlook

This work deals with the core phenomenology of the diphoton excess observed by the LHC experiments ATLAS and CMS around 750 GeV invariant mass. We consider both the case where the data is described by a narrow and a broad resonance. We obtained model-independent constraints on the allowed couplings and branching fractions to various final states, including the interplay with other existing bounds. Our findings suggest that the anomaly cannot be accounted for by the presence of a single additional singlet or doublet spin zero field and the Standard Model degrees of freedom; this includes all two Higgs doublet models. We prove that the whole parameter space of the MSSM is ruled out as an explanation for the excess by requiring the absence of charge and colour breaking minima. If we assume that the resonance is broad we find that it is challenging to find a weakly coupled explanation. However, we provide an existence proof in the form of a vectorlike model of quarks with exotic electric charge of $5/3$ or above. For the narrow resonance case a similar model with ordinary charges can be perturbative up to high scales. We also consider dilaton models, and they appear to be inconsistent with the data, even if arbitrary extra contributions to the QED and QCD beta functions are allowed. As already mentioned, in all the scenarios studied by us we find that new particles below the TeV scale need to be present in addition to the resonance. They must have couplings to the scalar itself, to photons and to gluons and possibly also to light quarks. Further study of their LHC phenomenology would be interesting to follow. Based on our toy models, in which new resonance to the light quarks coupling can be present, an interesting linkage between flavor physics and the physics related to the resonance might be present.

Acknowledgments

GP is supported by the BSF, ISF, and ERC-2013-CoG grant (TOPCHARM # 614794). SJ thanks GP and the Weizmann Institute for hospitality, including during the period in which this paper was conceived. SJ acknowledges partial support from the UK STFC under Grant Agreement ST/L000504/1. SJ acknowledges the NExT Institute.

References

- [1] ATLAS Collaboration, “Search for resonances decaying to photon pairs in 3.2 fb^{-1} of pp collisions at $\sqrt{s} = 13 \text{ TeV}$ with the ATLAS detector,” Tech. Rep. ATLAS-CONF-2015-081, CERN, Geneva, Dec, 2015. <http://cds.cern.ch/record/2114853>.
- [2] CMS Collaboration, “Search for new physics in high mass diphoton events in proton-proton collisions at 13 TeV,” Tech. Rep. CMS-PAS-EXO-15-004, CERN, Geneva, 2015. <http://cds.cern.ch/record/2114808>.
- [3] L. D. Landau, “On the angular momentum of a system of two photons,” *Dokl. Akad. Nauk Ser. Fiz.* **60** no. 2, (1948) 207–209.
- [4] C.-N. Yang, “Selection Rules for the Dematerialization of a Particle Into Two Photons,” *Phys. Rev.* **77** (1950) 242–245.
- [5] CMS Collaboration, V. Khachatryan *et al.*, “Search for diphoton resonances in the mass range from 150 to 850 GeV in pp collisions at $\sqrt{s} = 8 \text{ TeV}$,” *Phys. Lett.* **B750** (2015) 494–519, [arXiv:1506.02301 \[hep-ex\]](https://arxiv.org/abs/1506.02301).
- [6] ATLAS Collaboration, G. Aad *et al.*, “Search for high-mass diphoton resonances in pp collisions at $\sqrt{s} = 8 \text{ TeV}$ with the ATLAS detector,” *Phys. Rev.* **D92** no. 3, (2015) 032004, [arXiv:1504.05511 \[hep-ex\]](https://arxiv.org/abs/1504.05511).
- [7] CMS Collaboration, “Search for High-Mass Diphoton Resonances in pp Collisions at $\sqrt{s}=8 \text{ TeV}$ with the CMS Detector,” Tech. Rep. CMS-PAS-EXO-12-045, CERN, Geneva, 2015. <http://cds.cern.ch/record/2017806>.
- [8] CMS Collaboration, “Search for Resonances Decaying to Dijet Final States at $\sqrt{s} = 8 \text{ TeV}$ with Scouting Data.”
- [9] CMS Collaboration, V. Khachatryan *et al.*, “Search for Resonant $t\bar{t}$ Production in Proton-Proton Collisions at $\sqrt{s} = 8 \text{ TeV}$,” [arXiv:1506.03062 \[hep-ex\]](https://arxiv.org/abs/1506.03062).
- [10] ATLAS Collaboration, G. Aad *et al.*, “Search for a high-mass Higgs boson decaying to a W boson pair in pp collisions at $\sqrt{s} = 8 \text{ TeV}$ with the ATLAS detector,” [arXiv:1509.00389 \[hep-ex\]](https://arxiv.org/abs/1509.00389).
- [11] CMS Collaboration, “Search for a standard model like Higgs boson in the H to ZZ to $l+l- q\bar{q}$ decay channel at $\sqrt{s}=8 \text{ TeV}$,” Tech. Rep. CMS-PAS-HIG-14-007, CERN, Geneva, 2015. <https://cds.cern.ch/record/2001558>.
- [12] CMS Collaboration Collaboration, “Search for di-Higgs resonances decaying to 4 bottom quarks,” Tech. Rep. CMS-PAS-HIG-14-013, CERN, Geneva, 2014. <http://cds.cern.ch/record/1748425>.
- [13] ATLAS Collaboration, G. Aad *et al.*, “Search for a new resonance decaying to a W or Z

boson and a Higgs boson in the $\ell\ell/\ell\nu/\nu\nu + b\bar{b}$ final states with the ATLAS detector," *Eur. Phys. J.* **C75** no. 6, (2015) 263, [arXiv:1503.08089 \[hep-ex\]](https://arxiv.org/abs/1503.08089).

[14] ATLAS Collaboration, G. Aad *et al.*, "Search for neutral Higgs bosons of the minimal supersymmetric standard model in pp collisions at $\sqrt{s} = 8$ TeV with the ATLAS detector," *JHEP* **11** (2014) 056, [arXiv:1409.6064 \[hep-ex\]](https://arxiv.org/abs/1409.6064).

[15] ATLAS Collaboration, G. Aad *et al.*, "Search for new resonances in $W\gamma$ and $Z\gamma$ final states in pp collisions at $\sqrt{s} = 8$ TeV with the ATLAS detector," *Phys. Lett. B* **738** (2014) 428–447, [arXiv:1407.8150 \[hep-ex\]](https://arxiv.org/abs/1407.8150).

[16] ATLAS Collaboration, G. Aad *et al.*, "Search for high-mass dilepton resonances in pp collisions at $\sqrt{s} = 8$ TeV with the ATLAS detector," *Phys. Rev. D* **90** no. 5, (2014) 052005, [arXiv:1405.4123 \[hep-ex\]](https://arxiv.org/abs/1405.4123).

[17] CMS Collaboration, S. Chatrchyan *et al.*, "Search for narrow resonances and quantum black holes in inclusive and b -tagged dijet mass spectra from pp collisions at $\sqrt{s} = 7$ TeV," *JHEP* **01** (2013) 013, [arXiv:1210.2387 \[hep-ex\]](https://arxiv.org/abs/1210.2387).

[18] CMS Collaboration, "Search for Heavy Resonances Decaying into bb and bg Final States in pp Collisions at $\sqrt{s} = 8$ TeV,"

[19] ATLAS Collaboration, "Search for New Phenomena in Dijet Mass and Angular Distributions from pp Collisions at $\sqrt{s} = 13$ TeV with the ATLAS Detector," [arXiv:1512.01530 \[hep-ex\]](https://arxiv.org/abs/1512.01530).

[20] CMS Collaboration, V. Khachatryan *et al.*, "Search for narrow resonances decaying to dijets in proton-proton collisions at $\sqrt{s} = 13$ TeV," [arXiv:1512.01224 \[hep-ex\]](https://arxiv.org/abs/1512.01224).

[21] W. D. Goldberger, B. Grinstein, and W. Skiba, "Distinguishing the Higgs boson from the dilaton at the Large Hadron Collider," *Phys. Rev. Lett.* **100** (2008) 111802, [arXiv:0708.1463 \[hep-ph\]](https://arxiv.org/abs/0708.1463).

[22] M. Spira, A. Djouadi, D. Graudenz, and P. M. Zerwas, "Higgs boson production at the LHC," *Nucl. Phys. B* **453** (1995) 17–82, [arXiv:hep-ph/9504378 \[hep-ph\]](https://arxiv.org/abs/hep-ph/9504378).

[23] A. Efrati, E. Kuflik, S. Nussinov, Y. Soreq, and T. Volansky, "Constraining the Higgs-Dilaton with LHC and Dark Matter Searches," *Phys. Rev. D* **91** no. 5, (2015) 055034, [arXiv:1410.2225 \[hep-ph\]](https://arxiv.org/abs/1410.2225).

[24] B. Bellazzini, C. Csaki, J. Hubisz, J. Serra, and J. Terning, "A Higgslike Dilaton," *Eur. Phys. J. C* **73** no. 2, (2013) 2333, [arXiv:1209.3299 \[hep-ph\]](https://arxiv.org/abs/1209.3299).

[25] B. Gripaios, A. Pomarol, F. Riva, and J. Serra, "Beyond the Minimal Composite Higgs Model," *JHEP* **04** (2009) 070, [arXiv:0902.1483 \[hep-ph\]](https://arxiv.org/abs/0902.1483).

[26] J. F. Gunion and H. E. Haber, "The CP conserving two Higgs doublet model: The Approach to the decoupling limit," *Phys. Rev. D* **67** (2003) 075019, [arXiv:hep-ph/0207010 \[hep-ph\]](https://arxiv.org/abs/hep-ph/0207010).

[27] G. C. Branco, L. Lavoura, and J. P. Silva, "CP Violation," *Int. Ser. Monogr. Phys.* **103** (1999) 1–536.

[28] D. Ghosh, R. S. Gupta, and G. Perez, "Is the Higgs Mechanism of Fermion Mass Generation a Fact? A Yukawa-less First-Two-Generation Model," [arXiv:1508.01501 \[hep-ph\]](https://arxiv.org/abs/1508.01501).

[29] J. M. Frere, D. R. T. Jones, and S. Raby, "Fermion Masses and Induction of the Weak Scale by Supergravity," *Nucl. Phys. B* **222** (1983) 11.

[30] J. P. Derendinger and C. A. Savoy, "Quantum Effects and $SU(2) \times U(1)$ Breaking in

Supergravity Gauge Theories,” *Nucl. Phys.* **B237** (1984) 307.

- [31] J. A. Casas and S. Dimopoulos, “Stability bounds on flavor violating trilinear soft terms in the MSSM,” *Phys. Lett.* **B387** (1996) 107–112, [arXiv:hep-ph/9606237](https://arxiv.org/abs/hep-ph/9606237) [hep-ph].
- [32] R. Rattazzi and U. Sarid, “The Unified minimal supersymmetric model with large Yukawa couplings,” *Phys. Rev.* **D53** (1996) 1553–1585, [arXiv:hep-ph/9505428](https://arxiv.org/abs/hep-ph/9505428) [hep-ph].
- [33] J. Hisano and S. Sugiyama, “Charge-breaking constraints on left-right mixing of stau’s,” *Phys. Lett.* **B696** (2011) 92–96, [arXiv:1011.0260](https://arxiv.org/abs/1011.0260) [hep-ph]. [Erratum: *Phys. Lett.* B719,472(2013)].
- [34] W. Altmannshofer, M. Carena, N. R. Shah, and F. Yu, “Indirect Probes of the MSSM after the Higgs Discovery,” *JHEP* **01** (2013) 160, [arXiv:1211.1976](https://arxiv.org/abs/1211.1976) [hep-ph].
- [35] M. Carena, S. Gori, I. Low, N. R. Shah, and C. E. M. Wagner, “Vacuum Stability and Higgs Diphoton Decays in the MSSM,” *JHEP* **02** (2013) 114, [arXiv:1211.6136](https://arxiv.org/abs/1211.6136) [hep-ph].
- [36] W. Altmannshofer, C. Frugueule, and R. Harnik, “Fermion Hierarchy from Sfermion Anarchy,” *JHEP* **12** (2014) 180, [arXiv:1409.2522](https://arxiv.org/abs/1409.2522) [hep-ph].
- [37] A. Djouadi, “The Anatomy of electro-weak symmetry breaking. II. The Higgs bosons in the minimal supersymmetric model,” *Phys. Rept.* **459** (2008) 1–241, [arXiv:hep-ph/0503173](https://arxiv.org/abs/hep-ph/0503173) [hep-ph].